VOL. 15, NO. 24, DECEMBER 2020 ISSN 1819-6608
ARPN Journal of Engineering and Applied Sciences

www.arpnjournals.com

OPTICAL PROPERTIES OF THE FREESTANDING (2,2) SINGLE-WALLED BORON NITRIDE NANOTUBE

Riri Jonuarti[1], Freddy Haryanto[2,3] and Suprijadi[2,3]
[1]Department of Physics, Universitas Negeri Padang, Jl. Prof. Dr. Hamka, Air Tawar Barat, Padang, Indonesia
[2]Department of Physics, Institut Teknologi Bandung, Jalan Ganesha, Bandung, Indonesia
[3]Research Center for Nanoscience and Nanotechnology, Institut Teknologi Bandung, Jalan Ganesa, Bandung, Indonesia
E-Mail: riri_jonuarti@fmipa.unp.ac.id

ABSTRACT

We present results of our calculations on the optical properties of the freestanding (2,2) singled-walled boron nitride nanotube (SWBNNT) using the density functional theory (DFT) and random phase approximation (RPA). Previous study shows that freestanding (2,2) SWBNNT holds a narrow band gap of 3.01 eV. Then, our optical calculations exhibit that freestanding (2,2) SWBNNT generates the main absorption peaks are in the ultraviolet (UV) energy ranges. Furthermore, the freestanding (2,2) SWBNNT can absorb light at longer wavelengths. It starts from the visible light until the ultraviolet type C (UVC). These findings offer a chance that material can be applied as a photocatalyst.

Keywords: optical calculations, absorption, RPA.

INTRODUCTION

Boron nitride nanotubes (BNNTs) and carbon nanotubes (CNTs) have similar structures [1-4]. BNNTs can be easily visualized as a rolled up graphite sheet, where all C atoms are replaced by B and N atoms [5-9]. Furthermore, similar to CNTs, BNNTs also have high thermal conductivity and high strength [10]. However, it is more difficult to fabricate BN- NTs compared to CNTs. So far, BNNTs have been success- fully fabricated with diameters of 2.5-50 nm [11-17] with various possible applications such as dyeable fibers, superstrong composites, catalysis, chemical filtering, and storage of gases [18, 19]. These applications utilize BNNTs since these materials possess the insulating behavior with a band gap $\sim$6 eV [20, 21].

On the other hand, BNNTs also have varied narrow band gap that depends on its geometry for diameter BNNTs smaller than 9.5 nm. Since the theoretical studies and the well-defined synthesis are still lacking for the narrow SWBN- NTs, these limitations make narrow SWBNNTs have not be- come attentive. However, the new interesting information can be found by investigating these narrow SWBNNTs as a new photocatalyst. We should activate the photochemical reaction of SWBNNTs not only at the UV light energy range but also at energy ranges of the visible light using these narrow SWBNNTs. Because of this reason, we are interested in investigating the optical properties of the freestanding (2,2) SWBNNT using the random phase approximation (RPA).

RPA is a step in the transformation to simplify the many- electron Hamiltonian of a uniform electron gas to a quasi- electrons Hamiltonian in the context of plasma theory [22] which is first introduced by Bohm and Pines [23]. Then, this method is used to study the linear optical response of semi-conductors for the group-IV materials Si, SiC, and diamond by Gavrilenko *et al*. [24]. RPA is also employed by Rani *et al*. [25] to calculate the dielectric function, absorption spec- trum and energy loss-function of single layer graphene sheet. Considering that the RPA method has been widely used and has a good accuracy for optical calculations especially for narrow-gap systems, so the use of this method on our work is an appropriate decision.

COMPUTATIONAL DETAILS

Here, we consider the freestanding (2,2) SWBNNT constructed from the hexagonal boron nitride (h-BN) structure. We optimize the h-BN structure and then rolling it up to be- come the freestanding (2, 2) BNNT structure as shown in Figure-1. The optimization and relaxation of the structure are then carried out using the density functional theory (DFT) method until the convergence criteria are fulfilled: (a) the total (free) energy change between two steps are smaller than 10^{-6} a.u. for whole the break condition self-consistency (SC)-loop, (b) all the atomic forces for the atoms (or the allowed relaxed degrees of freedom) are smaller than -0.01 a.u. between two ionic steps relaxation [26]. Then, we use 1×1×16 k-point mesh and 450 eV of cut-off energy. In addition, the ion-electron interactions are described by the ultra-soft pseudopotentials [27-29], and exchange-correlation potential is described by the local density approximation (LDA) [30]

Hereinafter, we investigate the optical properties such as absorption, reflection, and transparency sections of the free- standing (2, 2) SWBNNT by computing its dielectric function using the random phase approximation (RPA). The di- electric function consisting of a real part and an imaginary part ($\varepsilon = \varepsilon_1 + i\varepsilon_2$), each of the parts will interpret the refractive index and the absorption of the freestanding (2, 2) SWBNNT.

RESULTS AND DISCUSSIONS

Optimized Structure and Band Gap

We first calculate the geometrical structure of hexagonal boron nitride (h-BN) before we construct the freestanding (2, 2) armchair SWBNNT. We get 0.1438 nm of B-N bond length from the optimized h-BN structure.

This B-N bond length value can be compared with previous value for B-N bond length, 0.1437 nm [31] and 0.1446 nm [32]. Then, we roll the optimized h-BN into the freestanding (2, 2) SWBNNT where a unit cell consisted of four boron and four nitrogen atoms.

We find that freestanding (2,2) SWBNNT has two dis- similar diameters (d_1 and d_2) and two dissimilar B-N bond lengths (r_1 and r_2) as illustrated in Fig. 1. The diameter of nitrogen ring (d_2 = 0.304 nm) is larger than the diameter of boron ring (d_1 = 0.267 nm). The B-N bonds along the tube axis (r_2 = 0.148 nm) are larger than the B-N bonds around the tube axis (r_1 = 0.146 nm). The lattice constant (c) is fix to be 0.257 nm. The freestanding (2,2) SWBNNT is expected to be stable with -52,36 eV of binding energy.

We also compare the calculated structural parameters of the freestanding (2, 2) SWBNNT in this work with other previous studies as shown in Table 1. Based on the data shown in Table 1, we conclude that the DFT-LDA do not underestimate the structure parameter of the freestanding (2,2) SWBNNT.

Then, we need the ground state calculation of the free- standing BNNT using DFT method as an input of the RPA calculation. Then, we also get the band structure diagram as shown in Fig. 2. The band gap of the freestanding (2, 2) SWBNNT is 3,01 eV of an indirect band gap. That indirect band gap occurred because the freestanding (2, 2) SWBNNT has a strong nearly free electron (NFE)–π^* hybridization which impact significantly in repulsion between the NFE and π^* band. It will make the π^* state moves closest to Z symmetry point while the π^* state is raised between Γ and Z symmetry point. In addition, that the NFE-π^* hybridization is proportional to the $\pi^* - \sigma^*$ hybridization. This hybridization impacts to the narrow band gap of the freestanding (2,2) SWBNNT.

Optical Properties

We group the optical spectra into three regions such as in- frared (IR) energy range from 0 to 1.7 eV, the visible light (VL) energy range 1.7 eV to 3.3 eV and the ultraviolet (UV) energy range > 3.3 eV. Furthermore, we divide the ultraviolet range into three groups, namely UVA (3.3 – 3.8 eV), UVB (3.8 – 4.4 eV), and UVC (4.4 - 12.4 eV) [33]. We deliberately divide those UV energy ranges to investigate which specific UV region the optical peaks of the SWBNNT are clearly visible.

Then, the dielectric function of the real part and the imaginary part of the freestanding (2, 2) SWBNNT for both light polarization directions are actually anisotropic. The peaks in the absorption spectra in case of light polarization perpendicular to the nanotube axis is higher than the peaks of light polarization parallel to the nanotube axis. Those peaks are not located in the same location for both light polarization directions. Furthermore, each figure of the real part and imaginary part of the dielectric function of the freestanding (2, 2) SWBNNT, consisted two graphs with local field (LF) effect and without local field (LF) effect as displayed in both Figure-3 and Figure-4. Both the dielectric function with LF effect and without LF effect have no significant contribution. The LF effect of the imaginary part of the freestanding (2,

2) SWBNNT dielectric function has lower absorption peaks than the absorption peaks of without LF effect of the imaginary part of the freestanding (2, 2) armchair SWBNNT. The LF effect corrections do not alter the prominent peak positions, but that effect just very slightly shifts the peaks to the higher energy spectra. In addition, either with LF effect or without LF effect corrections display the real part graphs of the dielectric function which started and ended at the same point for light polarization perpendicular and parallel to the nanotube axis as shown in Figure-4 (a) and Figure-4 (b).

Furthermore, we show the optical absorption of the free- standing (2, 2) SWBNNT for both light polarization perpendicular and parallel to the nanotube axis are provided in Figure-3(a) and Figure-3(b). From these figures, the absorption is started in the energy range of VL and then rise rocketed until UV energy region. Then, we discover the maximum peaks of the optical absorption around 6 eV for light polarization perpendicular to the nanotube axis, and around 5 eV in case of light polarization parallel to the nanotube axis.

Based on the absorption spectra of the freestanding (2,2) SWBNNT, we conclude that the freestanding (2,2) SWBNNT does not relate to its electronic bad gap. Since the previous study shows the band gap of the freestanding (2,2) SWBNNT is around 3,01 eV, the main absorption peaks should be in the range of UVA. However, the imaginary dielectric function graph indicates that the primary absorption peaks of the freestanding (2,2) SWBNNT are defined at UVC.

In addition, there are no peaks exist in the energy range of infrared (IR) as observed in all Figure-3. It means that there is no radiation absorptions occur in the IR section. It is caused by a very small or zero extinction coefficient (k) which is related to absorption in the IR energy ranges as displayed by $\varepsilon^{(2)} = 0$ in Figure-3. On the other hand,

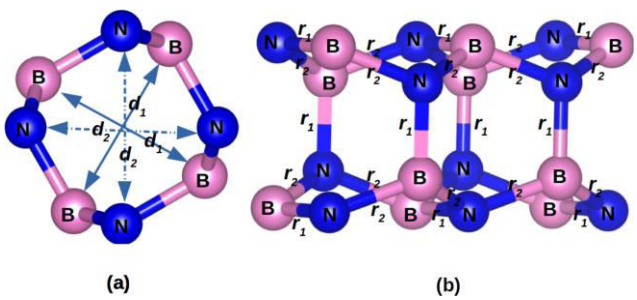

Figure-1. Geometry and structural parameters of freestanding (2, 2) SWBNNT; (a) along the rube axis and (b) side view. (B: boron as shown in pink and N: nitrogen as shown in blue).

Table-1. Structural parameters of the freestanding (2, 2) SWBNNT (nm).

	r_1	r_2	d_1	d_2	c
LDA (This work)	0.1460	0.1479	0.2672	0.3039	0.2568
PBE (Jia *et al.*) Ref. [47]	0.1464	0.1465	0.2685	0.3057	0.2524

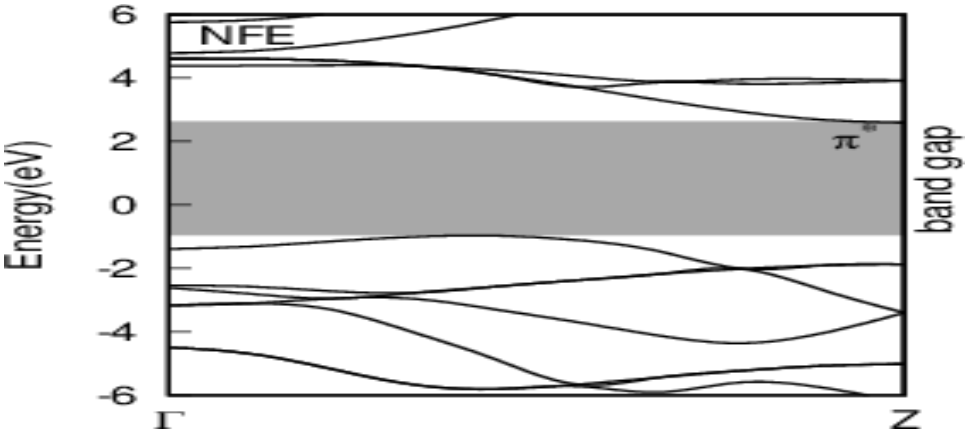

Figure-2. Band structure of the freestanding (2, 2) SWBNNT.

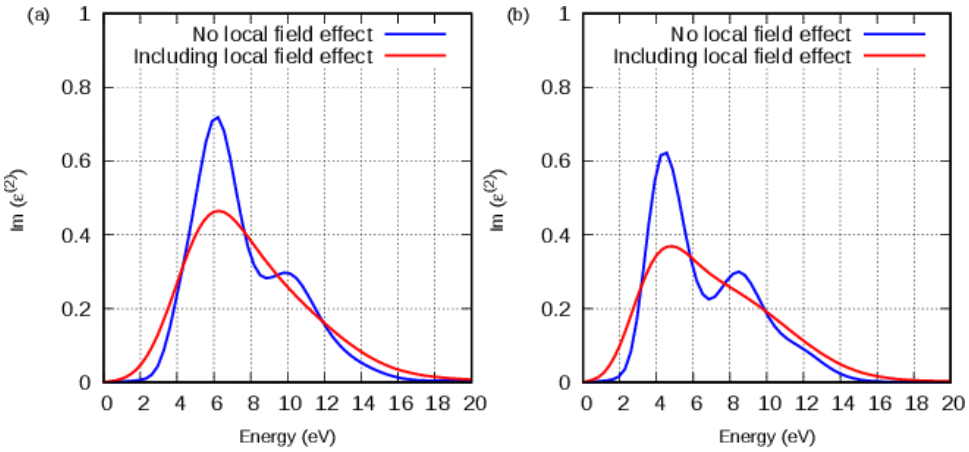

Figure-3. Imaginary part (a. u.) of the freestanding (2, 2) SWBNNT dielectric function (a) perpendicular (b) parallel to the tube axis

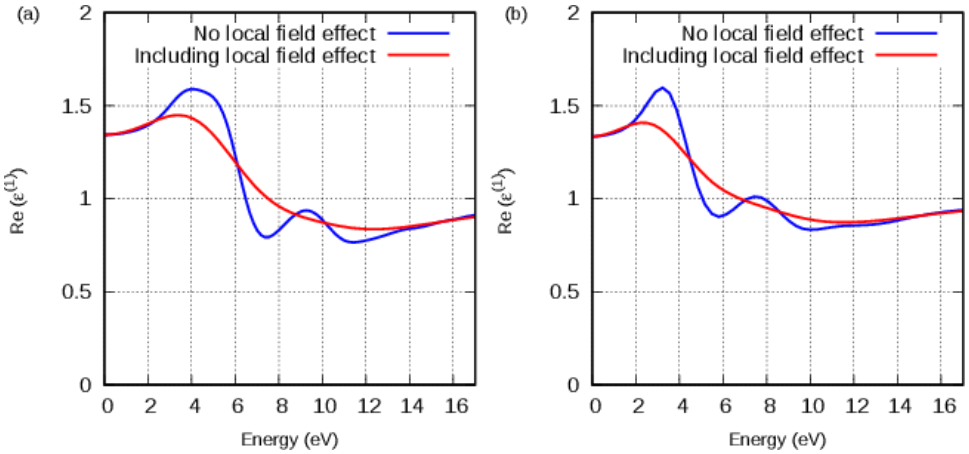

Figure-4. Real part (a. u.) of the freestanding (2, 2) SWBNNT dielectric function (a) perpendicular (b) parallel to the tube axis.

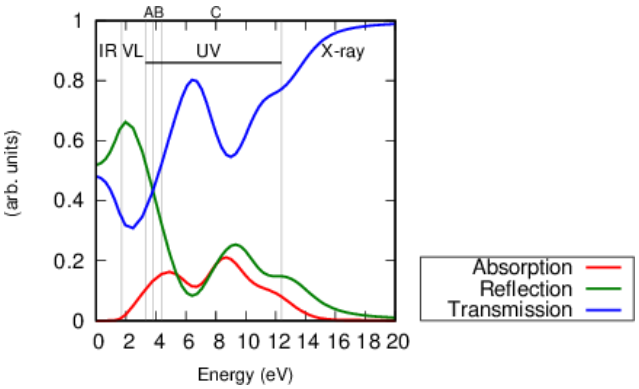

Figure-5. Light absorption, reflection and transmission on the freestanding (2,2) SWBNNT.

the refractive index (n) is high in those energy ranges by noticing $\varepsilon^{(1)} > 1$ in the IR and VL sections in Figure-4. Then, the correlation among $\varepsilon^{(1)}$, $\varepsilon^{(2)}$, n, and k are illustrated by:

$$\varepsilon^{(2)} = 2nk = 0 \quad (1)$$

$$\varepsilon^{(1)} = n^2 - k^2 > 1 \quad (2)$$

In case of k= 0, n >1, so:

$$\varepsilon^{(1)} = n^2 \quad (3)$$

Based on equation 3, the refractive index (n) in this case is root of $\varepsilon^{(1)}$ and the value of $\varepsilon^{(1)}$ at zero energy is called the dielectric constant. Thus, we have the dielectric constant values in case of light polarization perpendicular to the nanotube axis is 1.33 a.u., while in case of light polarization parallel to the nanotube axis is 1.34 a.u. as shown in Figure-4(a) and Figure-4(b). Such values mean that the light rate is 1.33 or 1.34 times lower when the freestanding (2.2) SWBNNT is penetrated than the light rate in the vacuum

The additional information of the optical properties of the freestanding (2,2) SWBNNT is provided by Figure-5. Since the total of absorption, reflection and transmission of light occurred on the freestanding (2,2) SWBNNT is 1 (A+R+T=1), we can find out which one of among the three of those activities more dominant takes place on this material. In general, most of the light is transferred by this material (high transmission) especially in the energy range which started from X-ray spectra to the higher energy spectra. In this area, the freestanding (2,2) SWBNNT is almost 100 % transparent. This transparency also occurred in the IR energy spectra, which is indicated by none the absorption occurred in the IR spectra. However, the freestanding (2,2) is not fully transparent in that IR range because some of the IR will be reflected as shown in Figure-5.

We also focus on the UV energy spectra which is divided into three subsections such as UVA, UVB and UVC. The calculation results indicate that the amount of the light absorption is slightly going up to around 18 % from the UVA to the UVB sections. The light will also be reflected and transmitted by the freestanding (2,2) SWBNNT. In this area, the amount of the reflection is equal to the transmission, but the amount of the reflection is going down from the UVA to the UVB. Furthermore, the transmission is going up from the UVA to the UVB and is rocketing to the UVC spectra. So that, the freestanding (2,2) SWBNNT creates the highest transparency in the UVC (5-8 eV) and high absorption in that UVC area.

Furthermore, the application of the freestanding (2,2) BNNT as a photocatalyst material needs to be stated based on these optical calculation especially for absorption activities. In order for a photocatalyst to work, it should be photactive. In that case, we need to specify the source of our photons are UV light and visible light. So that, the absorption activities of the freestanding (2,2) SWBNNT which started from visible light until UVC area, make this freestanding (2,2) SWBNNT has an opportunity for this application.

CONCLUSIONS

In summary, the anisotropic optical dielectric function of the freestanding (2, 2) SWBNNT is calculated using the random phase approximation (RPA) for light polarization perpendicular and parallel to the nanotube axis. The results of the calculations indicate that the maximum absorption and reflective peaks of the freestanding (2,2) SWBNNT demonstrate in the range of UV energy spectra and IR energy spectra. Hence, based on these optical calculations, we can relate that the freestanding (2,2) SWBNNT has absorption activities start from the visible light energy range until the UV energy range can be applied as a photocatalyst.

ACKNOWLEDGMENTS

Authors acknowledge the Physics department of Universitas Negeri Padang. Authors also thank to the support of the Chief of the Advanced Computational Physics Laboratory, Institut Teknologi Bandung (ITB).

REFERENCES

[1] Y. Wang, Y. Yamamoto, H. Kiyono and S. Shi- mada. 2008. Highly Ordered Boron Nitride Nanotube Arrays with Controllable Texture from Ammonia Borane by Template-Aided Vapor-Phase Pyrolysis. Journal of Nanomaterials, 2008.

[2] S. P. Ju, Y. C. Wang and T. W. Lien. 2011. Tuning the electronic properties of boron nitride nanotube by mechanical uni-axial deformation: a DFT study. Nanoscale Research Letters. 6(1): 160.

[3] S. Dolati, A. Fereidoon and K. R. Kashyzadeh. 2012. A Comparison Study between Boron Nitride Nanotubes and Carbon Nanotubes. International Journal of Emerging Technology and Advanced Engineering. 2.

[4] Y. S. Buranova, B. A. Kulnitskiy, I. A. Perezhogin and V. D. Blank. 2015. Structure of boron nitride nanotubes. Crystallography Reports. 60(1): 90-94.

[5] N. G. Chopra, R. J. Luyken, K. Cherrey, V. H. Crespi, M. L. Cohen, S. G. Louie and A. Zettl. 1995. Boron-Nitride Nanotubes. Science. 269: 966-967.

[6] Loiseau, F. Willaime, N. Demoncy, G. Hug and H. Pascard. 1996. Boron Nitride Nanotubes with Reduced Numbers of Layers Synthesized by Arc Discharge. Phys. Rev. Lett. 76: 4737-4740.

[7] M. Terrones, W. K. Hsu, H. Terrones, J. P. Zhang, S. Ramos, J. P. Hare, R. Castillo, K. Prassides, A. K. Cheetham, H. W. Kroto and D. R. M. Walton. 1996. Metal particle catalysed production of nanoscale BN struc-tures. Chemical Physics Letters. 259(5): 568-573.

[8] D. Golberg, Y. Bando, M. Eremets, K. Takemura, K. Kurashima and H. Yusa. 1996. Nanotubes in boron nitride laser heated at high pressure. Applied Physics Letters. 69(14).

[9] D. Golberg, Y. Bando, C.C. Tang and C.Y. Zhi. 2007. Boron Nitride Nanotubes. Advanced Materials. 19(18).

[10] C. Zhi, Y. Bando, C. Tang and D. Golberg. 2005. Immobiliza- tion of Proteins on Boron Nitride Nanotubes. Journal of the American Chemical Society. 127(49): 17144-17145.

[11] Y. Jun, Y. Dehong, C. Ying, C. Hua, L. Meng-Yeh, C. Bing-Ming, L. Jia and D. Wenhui. 2009. Narrowed bandgaps and stronger excitonic effects from small boron nitride nanotubes. Chemical Physics Letters. 476(4): 240-243.

[12] C. Tang, Y. Bando and T. Sato. 2002. Catalytic growth of boron nitride nanotubes. Chemical Physics Letters. 362(3): 185-189.

[13] C. Tang, Y. Bando, T. Sato and K. Kurashima. 2002. A novel precursor for synthesis of pure boron nitride nanotubes. Chem. Commun. pp. 1290-1291.

[14] C. Zhi, Y. Bando, C. Tan and D. Golberg. 2005. Effective pre- cursor for high yield synthesis of pure BN nanotubes. Solid State Communications. 135(1-2): 67-70.

[15] Y. Huang, J. Lin, C. Tang, Y. Bando, C. Zhi, T. Zhai, B. Dierre, T. Sekiguchi and D. Golberg. Bulk synthe-sis, growth mechanism and properties of highly pure ul- trafine boron nitride nanotubes with diameters of sub- 10 nm. Nanotechnology, 22(14):145602, 2011.

[16] L. Li, X. Liu, L. H. Li and Y. Chen. High yield BN-NTs synthesis by promotion effect of milling-assisted precursor. Microelectronic Engineering, 110:256–259, 2013.

[17] M. Yamaguchi, A. Pakdel, C. Zhi, Y. Bando, D. M. Tang, K. Firestein, D. Shtansky and D. Golberg. Uti-lization of multiwalled boron nitride nanotubes for the reinforcement of lightweight aluminum ribbons. Nanoscale research letters, 8:3, 2013.

[18] M. W. Smith, K. C. Jordan, C. Park, J. W. Kim, P. T. Lillehei, Crooks Roy and J. S Harrison. 2009. Very long single- and few-walled boron nitride nanotubes via the pressurized vapor/condenser method. Nanotechnology. 20(50): 505604.

[19] M. L. Cohen and A. Zettl. 2010. The physics of boron nitride nanotubes. Physics Today. 63(11): 34

[20] A. Rubio, J. L. Corkill and M. L. Cohen. 1994. Theory of graphitic boron nitride nanotubes. Phys. Rev. B. 49: 5081-5084.

[21] X. Blase, A. Rubio, S. G. Louie and M. L. Cohen. 1994. Stability and Band Gap Constancy of Boron Nitride Nanotubes. EPL (Europhysics Letters). 28(5): 335-340.

[22] Guo P. Chen, Vamsee K. Voora, Matthew M. Agee, Sree Ganesh Balasubramani, and Filipp Furche. 2017. Random-Phase Approximation Methods. Annual Re-view of Physical Chemistry. 68(1): 421-445.

[23] David Bohm and David Pines. 1953. A Collective Description of Electron Interactions: III. Coulomb Interactions in a Degenerate Electron Gas. Phys. Rev. 92: 609-625.

[24] V. I. Gavrilenko and F. Bechstedt. 1997. Optical functions of semiconductors beyond density-functional theory and random-phase approximation. Phys. Rev. B. 55: 4343-4352.

[25] P. Rani, G. S Dubey and V. K. Jindal. 2014. DFT study of op- tical properties of pure and doped Graphene. Physica E Low-dimensional Systems and Nanostructures. 62: 28-35.

[26] G. Kresse and J. Furthmüller. 1996. Efficient iterative schemes for ab initio total-energy calculations using a plane-wave basis set. Phys. Rev. B. 54:11169-11186.

[27] J. P. Perdew and A. Zunger. 1981. Self-interaction correction to density-functional approximations for many-electron systems. Phys. Rev. B. 23: 5048-5079.

[28] D. Vanderbilt. 1990. Soft self-consistent pseudopotentials in a generalized eigenvalue formalism. Phys. Rev. B. 41: 7892-7895.

[29] G. Kresse G and J. Hafner. 1994. Norm-conserving and ultrasoft pseudopotentials for first-row and transition elements. Journal of Physics: Condensed Matter. 6(40): 8245.

[30] G. Kresse, M. Marsman and J. Furthmüller. 2018. VASP the GUIDE. In VASP the GUIDE, Computational Materials Physics, Sensengasse 8/12, A-1090 Wien, Austria, October. Faculty of Physics, Universität Wien, Vienna.

[31] J. F. Jia, H. S. Wu, and H. Jiao. 2006. The structure and electronic property of BN nanotube. Physica B. 381: 90-95.

[32] R. W. Lynch and H. G. Drickamer. 1996. Effect of High Pressure on the Lattice Parameters of Diamond, Graphite, and Hexagonal Boron Nitride. The Journal of Chemical Physics. 44(1): 181-184.

[33] J. D'Orazio, S. Jarrett, A. Amaro-Ortiz and T. Scott. 2013. UV radiation and the skin. International Journal Molecular Sciences. 14: 12222-12248.